Proceedings of the ASME 2014 12th Biennial Conference on Engineering Systems Design and Analysis
ESDA2014
June 25-27, 2014, Copenhagen, Denmark

ESDA2014-20005

COMPUTATIONAL INVESTIGATIONS OF THERMAL SIMULATION OF SHELL AND TUBE HEAT EXCHANGER

Mahmoud Galal Yehia
Research Student of Mechanical Engineering,
Shoubra Faculty of Engineering, Benha University
Cairo, Egypt
medogalal@yahoo.com

Ahmed A. A. Attia
Assistant Prof. of Mechanical Engineering,
Shoubra Faculty of Engineering, Benha University
Cairo, Egypt
ahmed.attia@feng.bu.edu.eg

Osama Ezzat Abdelatif
Prof. of Mechanical Engineering, Shoubra Faculty of Engineering, Benha University
Cairo, Egypt
osama.abdellatif@feng.bu.edu.eg

Essam E. Khalil
Prof. of Mechanical Engineering, Cairo University
Cairo, Egypt
khalile1@asme.org

ABSTRACT

In the present paper, simulation for shell and tube heat exchanger investigated using CFD techniques. Numerical simulations of the turbulent, three-dimensional fluid flow and heat transfer are performed using Ansys Fluent 6.3. The effect of friction characteristics on the model of heat exchanger is discussed. A RNG κ-ε turbulence model with non-equilibrium wall function and 2nd order upwind is used. The present model is validated with the experimental literature and show a good agreement. The numerical results of the present study predict reasonably agree well with available correlations. Finally the present study model can be used to model a shell and tube heat exchanger with a satisfactory accuracy level in predictions.

Keywords: numerical simulation, shell and tube heat exchanger, turbulence model, validation study.

NOMENCLATURE

A	Area (m^2)
c_p	Pressure coefficient (J/kg.K)
D	Diameter (m)
f	Friction factor
h	Heat transfer coefficient ($W/m^2.K$)
h_i	Heat transfer coefficient for pure cross flow in ideal tube bank ($W/m^2.K$)
J_c	Segmental baffle window correction factor
J_l	Baffle leakage correction factor
J_b	Bypass correction factor, tube bundle to shell
J_s	Unequal inlet/outlet baffle spacing correction factor, applicable only if such differences exist
J_r	Laminar heat transfer correction factor, applicable for Re < 100
k	Thermal conductivity (W/m.K)
L	Length (m)
ṁ	Mass flow rate (kg/s)
Nu	Nusselt number
Pr	Prandtl number
Q	Heat transfer (W)
Re	Reynolds number
T	Temperature (K)
u	Velocity (m/s)
Δp	Pressure drop (pa)
Δp_c	Combined pressure drop of all the interior cross flow section (baffle tip to baffle tip) (pa)
Δp_w	Combined pressure drop in all the windows crossed (pa)
Δp_e	Pressure drop in the two end zones (pa)
ΔT	Temperature difference (K)
ρ	Density (kg/s)
μ	Dynamic viscosity (kg/m.s)
κ	Turbulence kinetic energy
ε	Dissipation rate

Subscripts

b	Bulk
c	Cross section
i	Inlet
o	Outlet
s	Shell side
sr	Surface
t	Tube side
w	Wall

1. INTRODUCTION

Heat exchangers are found in the power generation field, and in numerous industrial applications, such as the chemical and petroleum industry, nuclear plants, steam generation in a boiler or air cooling in the coil of an air conditioner. The shell and tube heat exchanger is the most versatile type of heat exchangers and is the one most widely used in these fields. That is due to their relatively simple construction and the multi-purpose application possibilities for gaseous and fluid media in a very large temperature and pressure range. This has led to increased levels of research experimentally, analytically and numerically on the heat transfer and hydraulic behavior of heat exchangers. [1]

2. LITRATURE SURVEY

2.1 EXPERIMENTAL INVESTIGATIONS

The experiments primary concern on the determination of overall heat transfer coefficient and Nusselt number as a direct index on heat exchanger performance. Also, one of their concerns is to determine the pressure drop and friction factor at different geometric arrangements.

Eiamsa–ard et al. [2] have investigated experimentally the effect of regularly–spaced dual twisted tapes with variable twist and space ratios in comparison with single and dual full-length twisted tapes. The tapes located into a uniform wall heated pipe. Heat transfer and friction characteristics of turbulent air flow at a Reynolds number range from 4000 to 19000 are investigated. An empirical correlation for Nusselt number and friction factor of a plain tube case aredeveloped as:

$$Nu = 0.017\,\mathrm{Re}^{0.82}\,\mathrm{Pr}^{0.4} \tag{1}$$

$$f = 3.1\mathrm{Re}^{-0.48} \tag{2}$$

Thianpong et al. [3] have investigated experimentally the effect of twisted tape with variable twist ratio, in a dimpled inner pipe of a counter flow double pipe heat exchanger with dimple variable pitch ratio. Heat transfer and friction characteristics of turbulent air flow at a Reynolds number range from 12000 to 44000 are investigated. An empirical correlation for Nusselt number and friction factor of the inner plain tube case are also given as:

$$Nu = 0.049\,\mathrm{Re}^{0.706}\,\mathrm{Pr}^{0.4} \tag{3}$$

$$f = 0.718\mathrm{Re}^{-0.309} \tag{4}$$

Chiu et al. [4] have investigated experimentally and numerically the effect of longitudinal strip inserts (both with and without holes) and twisted–tape inserts with three different twisted angles. The strips and tapes inserted in the tubes of a counter flow shell and tube heat exchanger. Heat transfer and friction characteristics of turbulent air flow at a Reynolds number range from 7000 to 42000 are investigated. The main conclusion is that both Nusselt number and pressure drop values for inserted strips and tapes are higher than those of plain tubes. The work done numerically using commercial CFD software.

2.2 ANALYTICAL INVESTIGATIONS

In the present paper, it was found that the analytical methods with its corresponding empirical correlations of heat transfer and friction have limitations and are of doubtful accuracy.

For the tube side flow's friction correlations, Moody correlation [5] for fully developed laminar flow, also Colebrook correlation [6] for fully developed turbulent flow. Petukhov correlation [7] for fully developed turbulent flow at $3000 \le \mathrm{Re} \le 5 \times 10^6$ is given as:

$$f \equiv (0.790\ln \mathrm{Re} - 1.64)^{-2} \tag{5}$$

For the tube side flow's heat transfer correlations, Keys correlation [8] for laminar flow with a constant surface temperature condition and the thermal entry length problem or combined entry length with $\mathrm{Pr} \ge 5$, Baehr and Stephan correlation [9] for the combined (thermal and velocity) entry problem, Sieder and Tate correlation [10] for the combined entry length laminar flow.

For turbulent flow heat transfer, Colburn correlation [11] for fully developed (hydro-dynamically and thermally) turbulent flow in a smooth circular tube is given as:

$$Nu = 0.023\,\mathrm{Re}^{4/5}\,\mathrm{Pr}^{1/3} \tag{6}$$

The Dittus-Boelter equation [12] for full developed turbulent flow, also, Sieder and Tate correlation [10] for fully developed turbulent flow with by large property variations. A more accurate but complex correlation developed by Petukhov [7] for fully developed turbulent flow, and Gnielinski correlation [13] for smooth tubes over a large Reynolds number range including the transition region.

For the shell side flow, Ayub [14] evaluates shell side heat transfer coefficient in a single segmental shell and tube heat exchanger with baffle cut varies 20 – 50%. Gaddis et al. [15] correlation for shell side pressure drop taking into account the influence of leakage and bypass streams. Kapale et al. [16] correlation for shell-side pressure drop incorporating the effect of pressure drop in inlet and outlet nozzles along with the losses in the segments created by baffles at Reynolds numbers lying between 10^3 and 10^5. Wills and Johnston correlation [17] for shell side pressure drop. Col et al. [18] as a further step, suggested a new procedure which extends the Wills and Johnston method [17] to the low Reynolds number range from 170 to 33,000 to get a better agreement with experimental data.

Kern correlations [19] for shell side heat transfer and pressure drop with a fixed baffle cut of (25%) and without

adequately account for baffle-to-shell and tube-to-baffle leakages gives a conservative results and is only suitable for the preliminary sizing.

In the other hand, Bell-Delaware correlations [20] are a very detailed method and are usually very accurate in estimating the shell side heat transfer coefficient and the pressure drop for common shell side geometric arrangements. The heat-transfer coefficient and pressure drop are estimated from correlations for flow over ideal tube-banks, and the effects of leakage, bypassing and flow in the window zone are allowed for by applying correction factors. Bell-Delaware method assumes that the flow rate and the thermo-physical properties of the shell-side fluid are specified; also shell-side geometrical parameters are known.

The correlation for shell-side heat transfer coefficient is:

$$h_s = h_i(J_c J_l J_b J_s J_r) \tag{7}$$

Where,

h_s The shell side heat transfer coefficient

h_i The heat transfer coefficient for pure cross flow in ideal tube bank

J_c The segmental baffle window correction factor

J_l The baffle leakage correction factor

J_b The bypass correction factor, tube bundle to shell

J_s The unequal inlet/outlet baffle spacing correction factor, applicable only if such differences exist

J_r The laminar heat transfer correction factor, applicable for Re < 100

The correlation for shell-side pressure drop is [20]:

$$\Delta p_s = \Delta p_c + \Delta p_w + \Delta p_e \tag{8}$$

Where as shown in figure 1,

Δp_s The total shell-side pressure drop excluding nozzles

Δp_c The combined pressure drop of all the interior cross flow section (baffle tip to baffle tip)

Δp_w The combined pressure drop in all the windows crossed

Δp_e The pressure drop in the two end zones

As a general conclusion, it can be said that correlation based approaches may indicate the existence of a weakness in design, but CFD simulations can also pin point the source and the location of the weakness. Using CFD, together with supporting experiments, may speed up the shell-and-tube heat exchanger design process and may improve the quality of the final design.

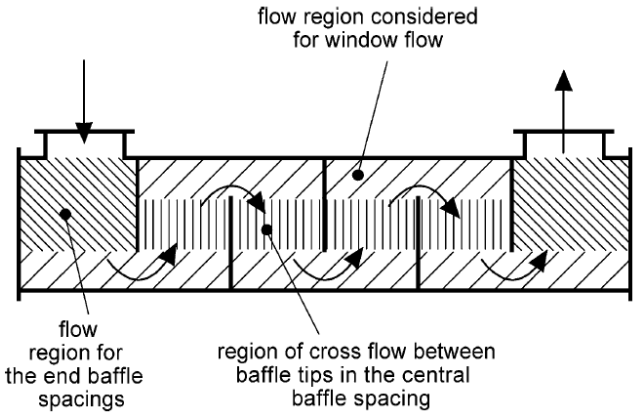

Fig. 1 The three components of the pressure drop (Δp_c, Δp_w, Δp_e) referred to the three flow zones. [18]

2.3 NUMERICAL INVESTIGATIONS

Ozden et al. [21] have investigated numerically using the commercial CFD package Fluent 6.3, the dependencies of the shell side geometrical parameters. The baffle spacing of 86, 62, 48, and 40 mm relative to number of baffles of 6, 8, 10, and 12, baffle cut ratio of 25% and 36% on the shell side heat transfer coefficient and the pressure drop at different shell side mass flow rate of 0.5, 1.0, and 2.0 kg/s.

The CFD simulations are performed for the shell side of a single tube pass shell and tube heat exchanger. Water is the shell side working fluid with inlet temperature of 300 K, and a constant tube wall temperature of 450 K.

The shell size inner diameter of 90 mm, length of 600 mm, tubes outer diameter of 20 mm, tube bundle geometry and pitch are triangular of 30 mm, number of tubes are 7 and the main conclusions from this investigation are as follows:

The κ–ε realizable turbulence model with first order discretization and the fine mesh of 1,360,000 elements is selected as the best simulation approach. For this heat exchanger geometry; 25% baffle cut gives slightly better results. Increasing the number of baffles would improve the heat transfer characteristics of the heat exchanger.

Also Ur-Rehman [22] has investigated using Fluent, the heat transfer coefficient and pressure drop of a un–baffled shell–and–tube heat exchanger and concluded that κ–ω SST model, with low Reynolds correction, provides better results as compared to other models.

From the foregoing review, the three–dimensional numerical analysis for the thermal–hydraulic characteristics of the flow inside heat exchangers is still needed more modification and coordination. The most of previous work was focusing on experimental way and developing the corresponding correlations. This less of researches has motivated the present study. Numerical simulations of the turbulent, three-dimensional fluid flow and heat transfer were performed using Ansys Fluent 6.3 and compared with the literature.

3. GOVERNING EQUATIONS AND TURBULENCE MODEL

Continuity Equation

$$\frac{\partial u}{\partial x}+\frac{\partial v}{\partial y}+\frac{\partial w}{\partial z}=0 \tag{9}$$

Momentum Equations

$$\rho\left(u\frac{\partial u}{\partial x}+v\frac{\partial u}{\partial y}+w\frac{\partial u}{\partial z}\right)=\rho g_x-\frac{\partial P}{\partial x}+\mu\left(\frac{\partial^2 u}{\partial x^2}+\frac{\partial^2 u}{\partial y^2}+\frac{\partial^2 u}{\partial z^2}\right) \tag{10}$$

in the x-dir.

$$\rho\left(u\frac{\partial v}{\partial x}+v\frac{\partial v}{\partial y}+w\frac{\partial v}{\partial z}\right)=\rho g_y-\frac{\partial P}{\partial y}+\mu\left(\frac{\partial^2 \upsilon}{\partial x^2}+\frac{\partial^2 \upsilon}{\partial y^2}+\frac{\partial^2 \upsilon}{\partial z^2}\right) \tag{11}$$

in the y-dir.

$$\rho\left(u\frac{\partial w}{\partial x}+v\frac{\partial w}{\partial y}+w\frac{\partial w}{\partial z}\right)=\rho g_z-\frac{\partial P}{\partial z}+\mu\left(\frac{\partial^2 w}{\partial x^2}+\frac{\partial^2 w}{\partial y^2}+\frac{\partial^2 w}{\partial z^2}\right) \tag{12}$$

in the z-dir.

Energy Equation

$$\rho c_v\left(u\frac{\partial T}{\partial x}+v\frac{\partial T}{\partial y}+w\frac{\partial T}{\partial z}\right)=\kappa\left(\frac{\partial^2 T}{\partial x^2}+\frac{\partial^2 T}{\partial y^2}+\frac{\partial^2 T}{\partial z^2}\right)+\phi \tag{13}$$

$$\phi=\mu\left[2\left(\frac{\partial u}{\partial x}\right)^2+2\left(\frac{\partial \upsilon}{\partial y}\right)^2+2\left(\frac{\partial w}{\partial z}\right)^2+\left(\frac{\partial \upsilon}{\partial x}+\frac{\partial u}{\partial y}\right)^2+\left(\frac{\partial w}{\partial y}+\frac{\partial v}{\partial z}\right)^2+\left(\frac{\partial u}{\partial z}+\frac{\partial w}{\partial x}\right)^2\right] \tag{14}$$

The RNG κ- ε Model

The RNG κ- ε model was derived using a rigorous statistical technique (called renormalization group theory). It is similar in form to the standard κ- ε model, but includes the following refinements:

- The RNG model has an additional term in its ε equation that significantly improves the accuracy for rapidly strained flows.
- The effect of swirl on turbulence is included in the RNG model which enhancing the accuracy for swirling flows.
- The RNG theory provides an analytical formula for turbulent Prandtl numbers, while the standard κ- ε model uses user-specified, constant values.
- While the standard κ- ε model is a high-Reynolds-number model, the RNG theory provides an analytically-derived differential formula for effective viscosity that accounts for low-Reynolds-number effects. Effective use of this feature does, however, depend on an appropriate treatment of the near-wall region.

These features make the RNG κ- ε model more accurate and reliable for a wider class of flows than the standard κ- ε model. [23]

The transport equations for the turbulence kinetic energy κ and its dissipation rate ε are:

$$\rho\frac{\partial k}{\partial t}+\rho U_i\frac{\partial k}{\partial x_i}=\frac{\partial}{\partial x_j}\left[\alpha_k\mu_{eff}\frac{\partial k}{\partial x_j}\right]+G_k+G_b-\rho\varepsilon-Y_M+S_K \tag{15}$$

$$\rho\frac{\partial \varepsilon}{\partial t}+\rho U_j\frac{\partial \varepsilon}{\partial x_j}=\frac{\partial}{\partial x_j}\left[\alpha_\varepsilon\mu_{eff}\frac{\partial \varepsilon}{\partial x_j}\right]+C_{1\varepsilon}\frac{\varepsilon}{k}(G_k+C_{3\varepsilon}G_b)-C_{2\varepsilon}\rho\frac{\varepsilon^2}{k}-R_\varepsilon+ \tag{16}$$

4. MODEL CONFIGURATION

The shell and tube heat exchanger model geometry presented in figure 2 was made exactly as Ozden et al. [21], were model main geometrical parameters are presented in table 1. The effect of baffle clearance, and tube to baffle bypass leakages are neglected.

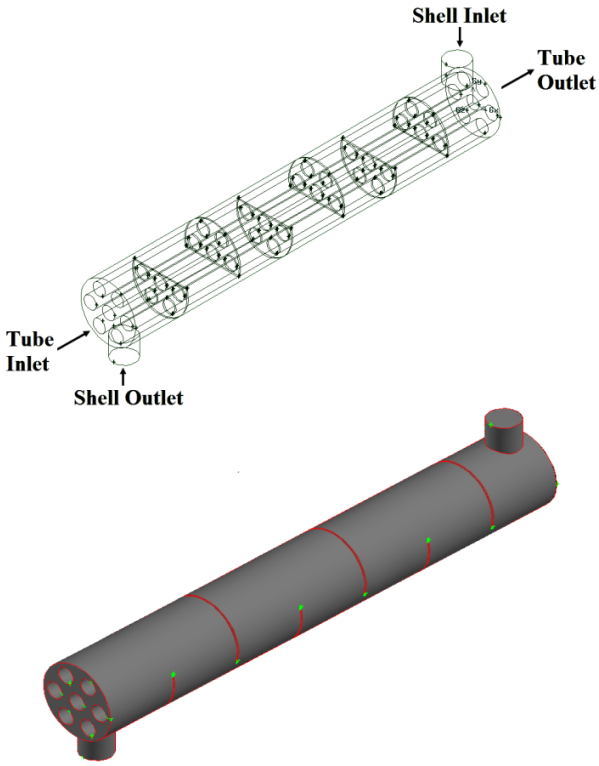

Fig. 2 Model configuration

Table 1 Model geometrical parameters

Description	Unit	Value
Shell diameter	mm	90
Shell inlet nozzle diameter	mm	36
Tube diameter	mm	20
Heat exchanger length	mm	600
No. of tube	--	7
Tube arrangement	--	Triangular 30º
No. of baffles	--	6
Baffle cut ratio	%	36

5. MODEL PROPERTIES

Tube side validation accomplished using model No. 1, while shell side validation accomplished using model No. 2, were both model properties are presented in table 2.

Table 2 Model properties

	Description	Symbol	Unit	Model No. 1	Model No. 2
Shell side	Working fluid	--	--	Water	Water
	Inlet mass flow rate	$\dot{m}_s$	kg/s	0.5 1.0 2.0	0.5 1.0 2.0
	inlet temperature	T_{si}	K	350	300
Tube side	Working fluid	--	--	Water	--
	Total inlet mass flow rate	$\dot{m}_t$	kg/s	0.5 1.0 2.0	-- -- --
	inlet temperature	T_{ti}	K	300	--
	Wall temperature	T_{tw}	K	--	450

6. MODEL SOLVER PARAMETERS

- Water is the working fluid with piecewise-linear profile for themo-physical properties between inlet hot and cold fluids.
- Shell and tube side outlet boundary conditions are pressure-outlet.
- Turbulence model: RNG κ-ε.
- Under-relaxation factors are Ansys Fluent defaults except energy and turbulent viscosity of 0.9.
- Pressure-velocity coupling is SIMPLE.
- Discretization schemes: 2nd order upwind.
- Wall cells type: triangle mesh face, volume cell type: tetrahedral mesh volume.

7. HEAT TRANSFER AND FRICTION CALCULATIONS

Tube Side Calculations

The tube side Reynolds number (Re_t) based on tubes inlet thermo-physical properties is

$$\mathrm{Re}_t = \frac{\rho_{t,i} u_{t,i} D_t}{\mu_{t,i}} \tag{17}$$

The tube side heat transfer coefficient (h_t) is

$$h_t = \frac{Q_t}{A_{t,sr}(T_{t,w} - T_{t,b})} \tag{18}$$

The heat absorbed by cold water in the tube (Q_t) is

$$Q_t = \dot{m}_t c_{p,t} \Delta T_t \tag{19}$$

Where $A_{t,sr}$ is the average tube surface area, $T_{t,w}$ is the tube average wall temperature, $T_{t,b}$ is the tube bulk temperature ($T_{t,i}+T_{t,o}/2$), $\dot{m}_t$ is the inlet mass flow rate ($\rho_{t,i}u_{t,i}A_{t,c}$), $c_{p,t}$ is the tube side pressure coefficient at tube bulk temperature, ΔT_t is the tube side temperature difference ($T_{t,o}-T_{t,i}$).

The tube side Nusselt number (Nu_t) at tube bulk temperature is

$$Nu_t = \frac{h_t D_t}{k_t} \tag{20}$$

The tube side friction factor (f_t) at tube bulk temperature is

$$f_t = \frac{\Delta p_t}{\left(\frac{L_t}{D_t}\right)\left(\frac{\rho_t u_{t,i}^2}{2}\right)} \tag{21}$$

Shell Side Calculations

The shell side outlet temperature ($T_{s,o}$) and the shell side pressure drop (Δp_s) are directly extracted from present study model. While the shell side heat transfer coefficient (h_s) was calculated by substitution of model geometrical parameters and output thermo-physical properties in the equations of Bell-Delaware method as detailed in ref. [20] to get each parameter value in equation (7) to finally get the value of the shell side heat transfer coefficient (h_s).

8. HEAT EXCHANGER GRID INDEPENDENCY CHECK

The numerical model should be tested for stability and robustness. This could only be achieved through comparisons for the same case but for different interval sizes to have very fine grid density. This would lead to attaining more accurate results. This specially true as it is very well known that the temperature and velocity variations are high near the wall solid body; therefore grid density should be very dense near the wall surface body where low grid density will affect the sensitivity of the calculations.

Therefore, four different mesh interval sizes were used to simulate the present case, with number of cells: 4,089,747 cells, 2,132,064 cells, 1,767,675 cells, and 1,534,864 cells relative to mesh volumes spacing internal size of 2, 3, 4, and 5 respectively, the results from this comparison are presented in figures 3 to 6.

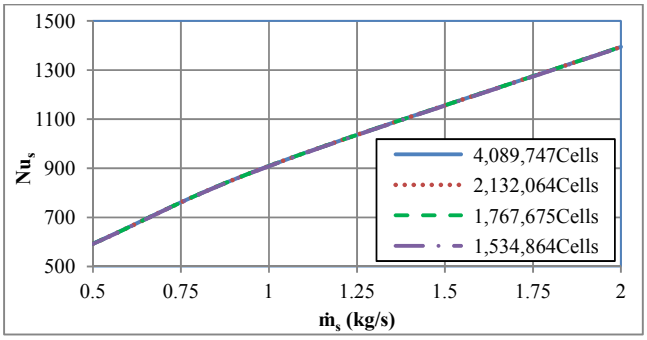

Fig. 3 Variation of shell side Nusselt number (Nu_s) with shell side inlet flow rate ($\dot{m}_s$) at different number of cells

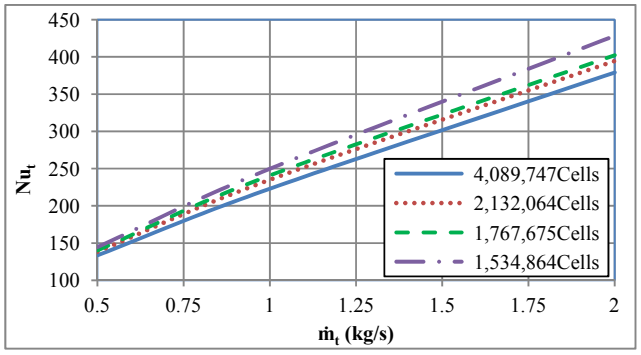

Fig. 4 Variation of tube side Nusselt number (Nu_t) with tube side inlet flow rate ($\dot{m}_t$) at different number of cells

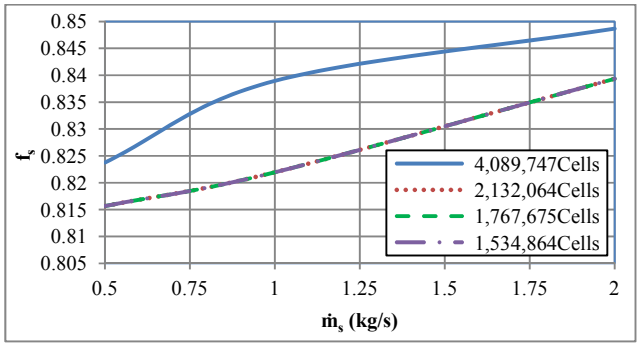

Fig. 5 Variation of shell side friction factor (f_s) with shell side inlet flow rate ($\dot{m}_s$) at different number of cells

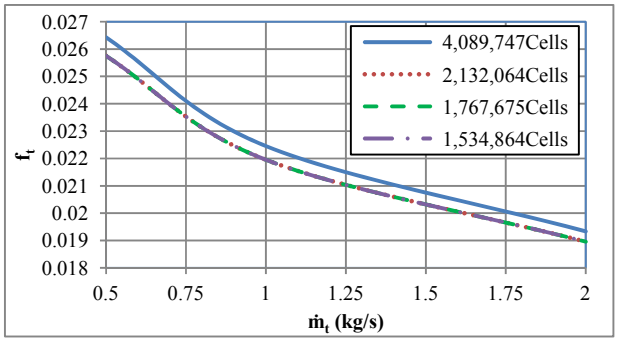

Fig. 6 Variation of tube side friction factor (f_t) with tube side inlet flow rate ($\dot{m}_t$) at different number of cells

From the shown figures 3 to 6 the change in number of cells from 2,132,064 to 1,534,864, do not have a noticeable effect in the results of tube and shell side Nusselt number and friction factor. But when increasing the number of cells to 4,089,747 the Nusselt number and friction factor deviate from the lesser density meshes, which mean that the solver is robust and sable within the value of 2,132,064 to 1,534,864.

So the model with 2,132,064 cells will be used which although it is the more dense, but to account for the required accuracy when we have to make some complications in the flow passage like putting any heat transfer enhancer, specially the selected mesh size was found to be suitable for the available computers facilities.

9. TURBULENCE MODELS VALIDATION

From the last section it can be concluded that the available range of mesh densities do not considerably affect on the heat transfer and friction results, so a further investigation is made to validate the available different turbulence models, and part of the obtained results are presented in this section for the validation of different turbulence models with the predictions of Ozden et al. [21] and Bell-Delaware analytical method [20].

The first level of turbulence model validation presented in figures 7 to 10, was for Standard, RNG and Realizable κ-ε models, κ-ω SST, and RSM with near-Wall Treatment of non-equilibrium wall functions, except κ-ω SST turbulence model which not support different near wall treatment functions.

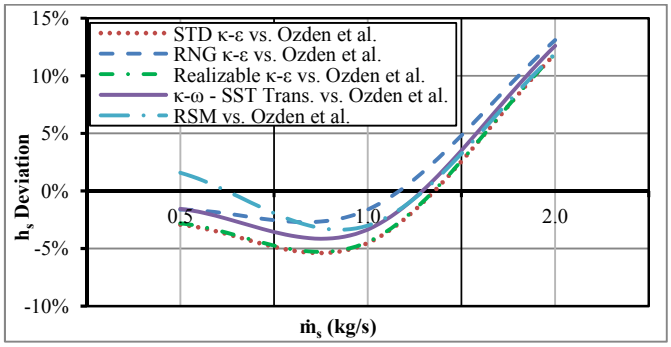

Fig. 7 Deviation of shell side heat transfer coefficient (h_s) predictions at various turbulence models from Ozden et al. predictions at different shell side mass flow rate ($\dot{m}_s$)

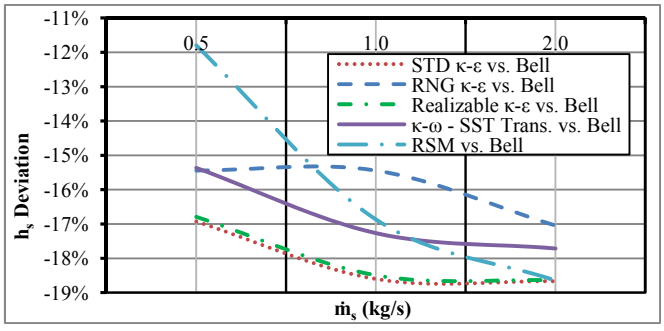

Fig. 8 Deviation of shell side heat transfer coefficient (h_s) predictions at various turbulence models from Bell-Delaware method at different shell side mass flow rate ($\dot{m}_s$)

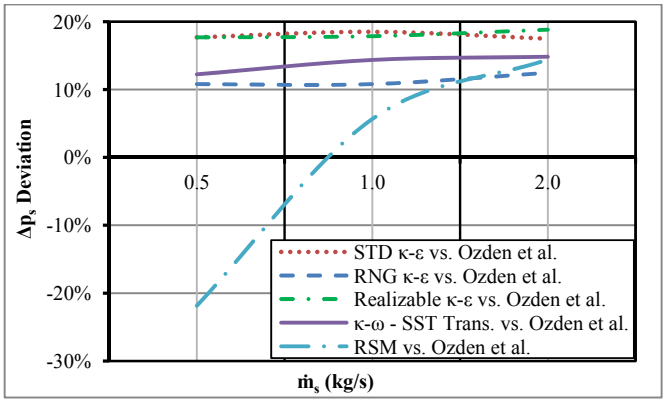

Fig. 9 Deviation of shell side pressure drop (Δp_s) predictions at various turbulence models from Ozden et al. predictions at different shell side mass flow rate ($\dot{m}_s$)

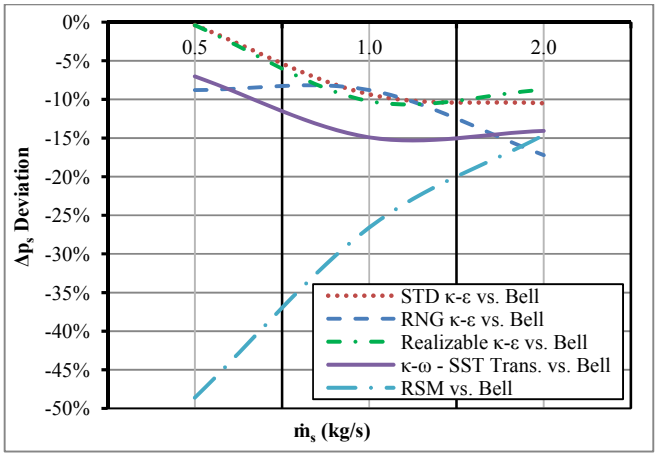

Fig. 10 Deviation of shell side pressure drop (Δp_s) predictions at various turbulence models from Bell-Delaware method at different shell side mass flow rate ($\dot{m}_s$)

The presented figures 7 to 10 show that although Realizable κ-ε model gives less deviation behavior from Bell-Delaware analytical method [20] for pressure drop results, but RNG κ-ε model show the best results for heat transfer in deviation with both Ozden et al. predictions [21] and Bell-Delaware analytical method [20], also the best results for pressure drop in deviation with Ozden et al. predictions [21]. Consequently the RNG κ-ε model with non-equilibrium wall functions, and 2nd order upwind discretization scheme is selected for a further investigation level.

The second level of turbulence model validation was between 1st order and 2nd order upwind discretization schemes for the best found turbulence model which is the RNG κ-ε model, as presented in figures 11 and 12.

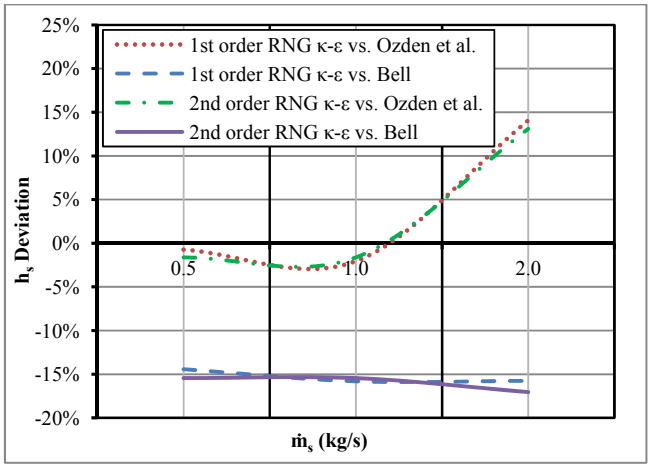

Fig. 11 Deviation of shell side heat transfer coefficient (h_s) predictions at both 1st order and 2nd order discretization schemes from Ozden et al. predictions and Bell-Delaware method at different shell side mass flow rate ($\dot{m}_s$)

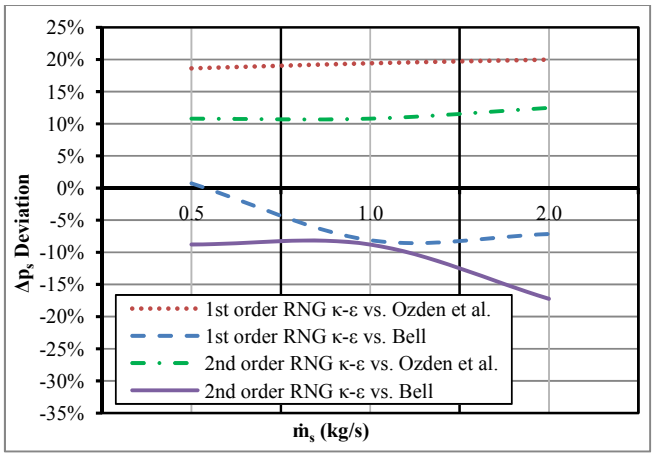

Fig. 12 Deviation of shell side pressure drop (Δp_s) predictions at both 1st order and 2nd order discretization schemes from Ozden et al. predictions and Bell-Delaware method at different shell side mass flow rate ($\dot{m}_s$).

The presented figure 11 shows that both 1st order and 2nd order upwind discretization schemes do not affect on the heat transfer predictions. While, the presented figure 12 shows that the 2nd order upwind gives the best results for pressure drop in deviation with Ozden et al. predictions [21]. Although the 1st order upwind show the best results for pressure drop in deviation with Bell-Delaware analytical method [20], but still the 2nd order RNG κ-ε model show the best results, as the enhancement in deviation with Ozden et al. predictions [21] for the 2nd order case is much more than the enhancement in deviation with Bell-Delaware analytical method [20] for the 2nd order case.

10. TUBE SIDE VALIDATION

Model No. 1 as presented in table 2 was used for the tube side validation of the shell and tube heat exchanger in compare with the following correlations:

Thianpong et al. [3] empirical correlation developed from the experimental results, were these experimental results was showing a maximum uncertainty in results of ± 10% for Nusselt number and ± 15% for friction factor, also a deviation of ± 7% for Nusselt number results in comparison with Dittus-Boelter correlation [12] and ± 18% for friction factor results in comparison with Blasius correlation [24].

Eiamsa-ard et al. [2] empirical correlations developed from the experimental results, were these correlations showing a maximum deviation of 6.7% for Nusselt number results in comparison with Colburn correlation [11], and a maximum deviation of 33.8% for friction factor results in comparison with Petukhov correlation [7].

The present tube side predictions in compare with the empirical correlations of Thianpong et al. [3], Eiamsa-ard et al. [2], Colburn [11] and Petukhov [7] at mass flow rate of 0.5, 1.0, and 2.0 kg/s relative to Reynolds number of 5319, 10637, and 21274 respectively are presented in figures 13 and 14.

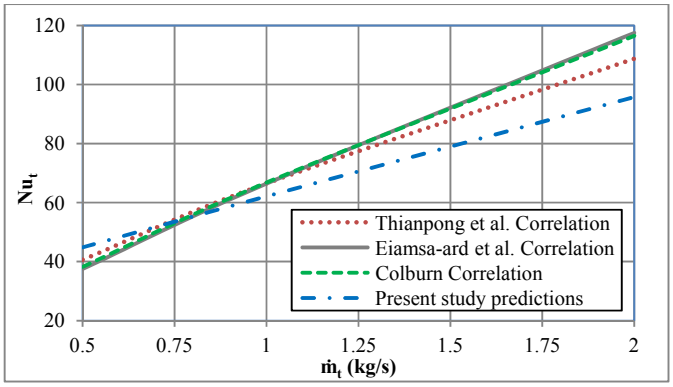

Fig. 13 Tube side Nusselt number as a function of mass flow rate for Present study predictions in compare with Thianpong et al. [3], Eiamsa-ard et al. [2] and Colburn [11] correlations

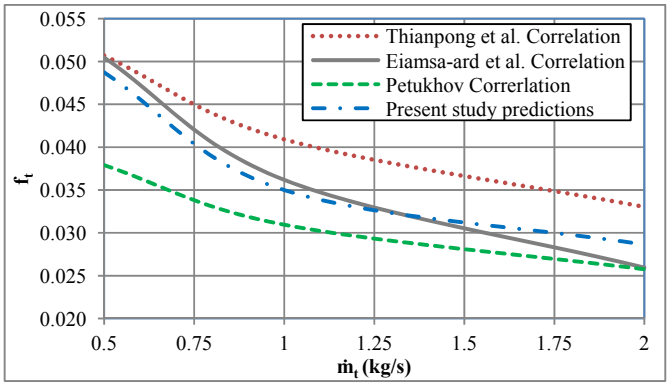

Fig. 14 Tube side friction factor as a function of mass flow rate for Present study predictions in compare with Thianpong et al., Eiamsa-ard et al. [2] and Petukhov [7] correlations

The results showing a maximum deviation of 11.9%, 19.7% and 17.8% for Nusselt number predictions in compare with the correlations of Thianpong et al. [3], Eiamsa-ard et al. [2], and Colburn [11] respectively.

While a maximum deviation of 14.5%, 10.4% and 28.6% for friction factor predictions in compare with the correlations of Thianpong et al. [3], Eiamsa-ard et al. [2], and Colburn [11] respectively.

11. SHELL SIDE VALIDATION

Model No. 2 as presented in table 2 was used for the shell side validation of the shell and tube heat exchanger with Ozden et al. predictions [21] and Bell-Delaware correlation [20].

Ozden et al. predictions [21] was showing a maximum deviation of 34.7% for heat transfer coefficient predictions in comparison with that of Bell-Delaware correlation [20], and a maximum deviation of 34.2% for pressure drop predictions in comparison with that of Bell-Delaware correlation [20].

The present study predictions for shell side of the shell and tube heat exchanger in compare with Ozden et al. predictions [21] and Bell-Delaware correlation [20] is presented in figures 15, 16 and 17.

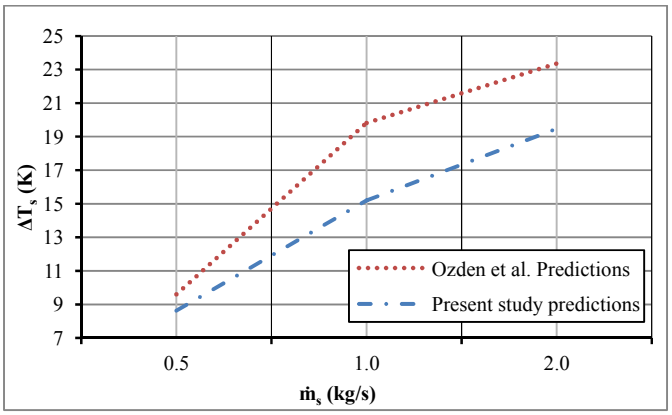

Fig. 15 Shell side temperature difference (ΔT_s) as a function of mass flow rate ($\dot{m}_s$) for present study predictions in compare with Ozden et al. predictions [21]

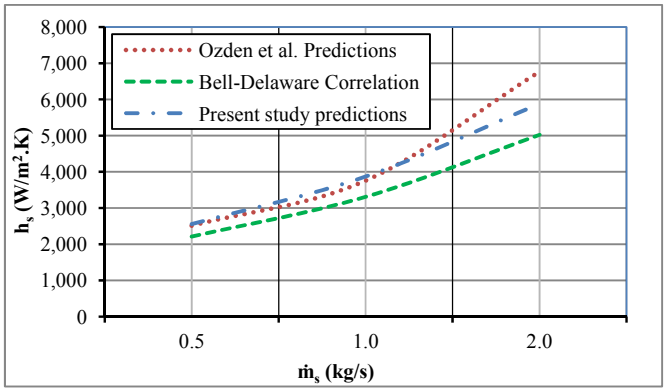

Fig. 16 Shell side heat transfer coefficient (h_s) as a function of mass flow rate ($\dot{m}_s$) for present study predictions in compare with Ozden et al. predictions [21] and Bell-Delaware correlation [20]

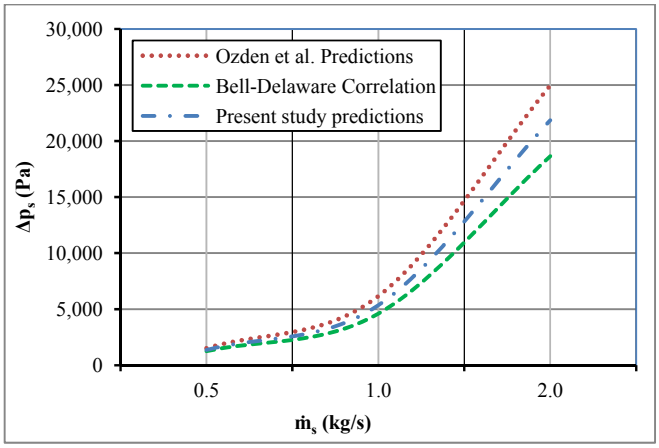

Fig. 17 Shell side pressure drop (Δp_s) as a function of mass flow rate ($\dot{m}_s$) for present study predictions in compare with Ozden et al. predictions [21] and Bell-Delaware correlation [20]

The results showing a maximum deviation of 23.3% for shell side temperature difference (relative to the same inlet temperature and 1.2% maximum deviation in the shell side outlet temperature in compare with Ozden et al. predictions [21]).

Also a maximum deviation of 14.1% and 15.8% for heat transfer coefficient predictions in compare with Ozden et al. predictions [21] and Bell-Delaware correlation [20], respectively.

While a maximum deviation of 20% and 8.1% for pressure drop predictions in compare with Ozden et al. predictions [21] and Bell-Delaware correlation [20].

Consequently, the results of the present study predictions reasonably agree well with literature predictions and correlations as it is laying between them although the deviation is increasing at high mass flow rates, which may occur due to that Ozden et al. used a different turbulence model (Realizable κ-ε model), different discretization scheme (1st order upwind), and different mesh size of 1,360,000 elements.

12. CONCLUSIONS

1- The number of cells of 2,132,064 cells relative to mesh volumes spacing internal size of 3, is the most robust and stable density (Fig. 3 to 6).

2- The RNG κ-ε model with non-equilibrium wall functions and 2nd order upwind discretization found to be the best turbulence model for the investigated case (Fig. 7 to 12).

3- Tube side Nusselt number match with different correlations but deviates to a maximum percentage of 19.7% at high Reynolds number (Fig. 13).

4- Although tube side friction factor predictions deviation reaches in some cases 28.6% but still the predictions is considered satisfactory as it is laying between different correlations results (Fig. 14).

5- A satisfactory deviation for the present predictions from Ozden et al. predictions for shell side temperature difference (Fig. 15).

6- Although heat transfer coefficient and pressure drop deviation reaches in some cases 15.8% and 20% respectively, but still the predictions is considered satisfactory as it is laying between Ozden et al. predictions and Bell-Delaware analytical method (Fig. 16 and 17).

7- Finally the present study model can be used to model a shell and tube heat exchanger with a satisfactory accuracy level in predictions.

REFERENCES

[1] Liang, C., and Papadakis, G., 2007, "Large Eddy Simulation of Cross-Flow through a Staggered Tube Bundle at Subcritical Reynolds Number", J. Fluids and Structures 23, pp. 1215 – 1230.

[2] Eiamsa–ard, S., Thianpong, C., Eiamsa-ard, P., and Promvonge, P., 2010, "Thermal characteristics in a heat exchanger tube fitted with dual twisted tape elements in tandem", J. Int. Communications in Heat and Mass Transfer, Vol. 37, Issue 1, pp. 39–46.

[3] Thianpong, C., Eiamsa-ard, P., Wongcharee, K., and Eiamsa-ard, S., 2009, "Compound heat transfer enhancement of a dimpled tube with a twisted tape swirl generator", J. International Communications in Heat and Mass Transfer 36, pp. 698–704.

[4] Chiu, Y. W., and Jang, J.Y., 2009, "3D numerical and experimental analysis for thermal–hydraulic characteristics of air flow inside a circular tube with different tube inserts", J. Applied Thermal Engineering 29, pp. 250-258.

[5] Moody, L. F., 1944, "friction factors for pipe flow", Transactions of the ASME, Vol. 66, pp. 671.

[6] Colebrook, C. F., 1939, "Turbulent flow in pipes with particular reference to the transition between the smooth and rough pipes laws", J. Institute of civil engineers London, Vol. 11.

[7] Petukhov, B.S., 1970, "Heat Transfer and Friction in Turbulent Pipe Flow with Variable Physical Properties". In: Irvine, T.F., Hartnett, J.P. (Eds.) Advances in Heat Transfer, vol. 6, Academic Press, New York, Cross Ref.

[8] Kays, W. M., 1955, "Numerical Solution for Laminar Flow Heat Transfer in Circular Tubes", Trans. ASME, vol. 77, pp. 1265–1274.

[9] Baehr, H.D. and Stephan, K., 2006, "Heat and Mass Transfer", 2nd Ed., Springer: Berlin, Heidelberg, New York.

[10] Sieder, E. N. and Tate, G.E., 1936, "Heat Transfer and Pressure Drop of Liquids in Tubes", Industrial & Engineering Chemistry J., 28, pp. 1429–1435.

[11] Colburn, A.P., 1933, "A Method of Correlating Forced Convection Heat Transfer Data and a Comparison with Liquid Friction", Trans. AIChE 29, pp. 174–210.

[12] Winterton, R. H. S., 1998, "Where did the Dittus and Boelter equation come from?", Int. J. Heat Mass Transfer, Vol. 41, Nos. 4-5, pp. 809-810.

[13] Gnielinski, V., 1976, "New Equations for Heat and Mass Transfer in Turbulent Pipe and Channel Flow", Int. Chem. Eng., 16, pp. 359–368.
[14] Ayub, Z. H., 2005, "A new chart method for evaluating single-phase shell side heat transfer coefficient in a single segmental shell and tube heat exchanger", J. Applied Thermal Engineering 25, pp. 2412–2420.
[15] Gaddis, E. S. and Gnielinski, V., 1997, "Pressure drop on the shell side of shell-and-tube heat exchangers with segmental baffles", J. Chemical Engineering and Processing 36, pp. 149-159.
[16] Kapale, U. C., and Chand, S., 2006, "Modeling for shell-side pressure drop for liquid flow in shell-and-tube heat exchanger", Int. J. of Heat and Mass Transfer, 49, pp. 601–610.
[17] Wills, M.J.N., Johnston, D., and Harwell, A., 1984, "A new and accurate hand calculation method for shell side pressure drop and flow distribution", 2nd National Heat Transfer Conference, HTD N. 36. New York, ASME, pp. 67–79.
[18] Col, D. D. Muzzolon, A., Piubello, P., and Rosetto, L., 2005, "Measurement and prediction of evaporator shell-side pressure drop", Int. J. Refrigeration, 28, pp. 320–330.
[19] Kern, D. Q., 1950, "Process Heat Transfer", McGraw-Hill, New York, Ch. 7.
[20] Bell, K. J., 1963, "Final Report of the Cooperative Research Program on Shell and Tube Heat Exchangers", Bull. No. 5, University of Delaware Engineering Experiment Station, New York.
[21] Ozden, E., and Tari, I., 2010, "Shell Side CFD Analysis of a Small Shell–and–Tube Heat Exchanger", J. Energy Conversion and Management 51, pp. 1004 – 1014.
[22] Ur-Rehman, U., 2011, "Heat Transfer Optimization of Shell–and–Tube Heat Exchanger through CFD Studies", M.Sc. Thesis Chalmers University of Technology, Göteborg, Sweden.
[23] Fluent 6.2 Documentation, © Fluent Inc. 2005.
[24] Incropera, F. P., DeWitt, D.P., Bergman, T.L., and Lavine, A.S., 2011, "Introduction to Heat Transfer", 6th Ed., John Wiley & Sons, Inc.